The Impact of Rotary Friction Welding on the Characteristics of Aluminum Composite Reinforced with Graphene Oxide

Mutlag Shafi Alaythee, Shabib Sulaiman Al Rashdi

College of Engineering, National University of Science and Technology, Sultanate of Oman.
Email: mutlagshafi@nu.edu.om

Aluminum composite materials are created by blending an aluminum alloy (AL-Si12Fe) base material with reinforcement elements that consist of 5% graphene oxide (GO). The components are fabricated using the stir-squeeze casting technique. A study was conducted to ascertain the mechanical properties of these composites. The results indicated that the inclusion of GO reinforcements significantly enhanced their strength. The AL-Si12Fe+5%GO and AL-Si12Fe+5%GO-weld composites exhibited a 41% and 57% increase in ultimate tensile strength (UTS) compared to the LM6 aluminum alloy. In addition, the ductility increased by 302% and 466% respectively when the rotary friction welding technique was used for welding. Rotary friction welding is a technique used to enhance and restructure crystals, as well as induce super-deformation.

Keywords: AL-Si12Fe alloy, aluminum composites, rotary friction welding, graphene oxide.

1. Introduction

The current study focuses on the potential application of friction welding for the purpose of connecting Aluminum Composite Materials (ACM). Aluminum alloys can be reinforced by including substances such as graphite or industrial waste, leading to the creation of Aluminum Matrix Composites (AMCs). This technique of reinforcing enhances the mechanical characteristics of the alloys. The increasing use of Advanced Composite Materials (ACMs) in the automotive and aerospace sectors has required the creation of effective techniques for connecting these materials [1].

Friction welding, specifically solid-state welding, is a preferred technique due to its low heat input, absence of filler materials, little heat impacted zones, reduced distortion and residual strains, and enhanced material qualities. Rotary friction welding (RFW) is highly suitable for aluminum alloys due to its ability to effectively match material properties with process capabilities [2].

Graphene is a monolayer of carbon atoms that are closely packed in a two-dimensional (2D) structure. It has a smooth surface and the carbon atoms are hybridized in a sp2 configuration. Graphene possesses distinctive characteristics as a result of its honeycomb structure, including its lightweight nature, transparency, and exceptional mechanical, thermal, and hardness qualities. Consequently, it finds applications in a diverse array of sectors [3]. The Hummers method, a widely used technique for oxidizing graphite, involves the use of substances such as H2SO4, HNO3, and KMnO4 to convert graphite into GO [4], similar to other methods based on the Hummers approach [5]. When exposed to various reducing agents, such as ascorbic acid, sodium borohydride, and hydrazine, graphite oxide will undergo chemical reduction. Typically, the final product is called reduced graphene oxide [6], as depicted in Figure 1.

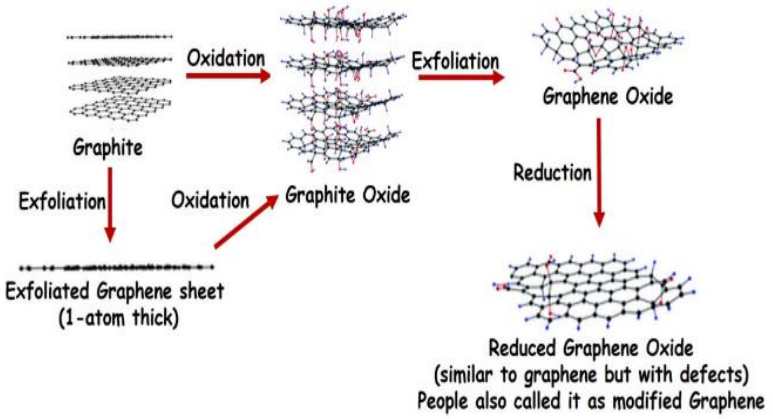

Figure 1. Strategies of Graphene Oxide via Hummer Method.

2. Methods and Methodology:

In this study, we will analyze the mechanical properties and microstructure of reinforcing elements used in aluminum composites. The blend of materials was made utilizing a combination of stir squeeze casting and the RFW process, and it contains 5% graphene oxide (GO). We will evaluate the properties of the final products. The GO powder with a thickness ranging from 1 to 5 nm is shown in Figure 2. The outcomes of the GO specification can be seen in Table 1, while the findings of the chemical composition analysis can be found in Table 2.

Figure 2. GO Powder.

Table 1. Specification of GO Powder.

Parameters	Value
Purity	>99%
Thickness (diameter)	1-5 nm
Number of layers	The average number of layers 4-8
Surface Area	210 m^2/g

Table 2. Chemical Composition of GO Powder.

Element	C	O	Na	S
Wt %	61.67	37.89	0.27	0.18

Employed the stir squeeze casting method to manufacture an Advanced Metal Composite (AMC). Figure 3 illustrates the utilization of hydraulic forging and casting procedures in the casting machine to merge and solidify materials. In order to avoid moisture and the agglomeration of particles, the preheater chamber of the stir squeeze casting machine elevated the temperature of the reinforcement particles to 300°C. Subsequently, the heated reinforcement particles were meticulously mixed with molten AL-Si12Fe metal for a specified duration to ensure a uniform distribution inside the matrix phase. The samples were created by subjecting the mixture to hydraulic pressure. Table 3 includes the specific settings for casting.

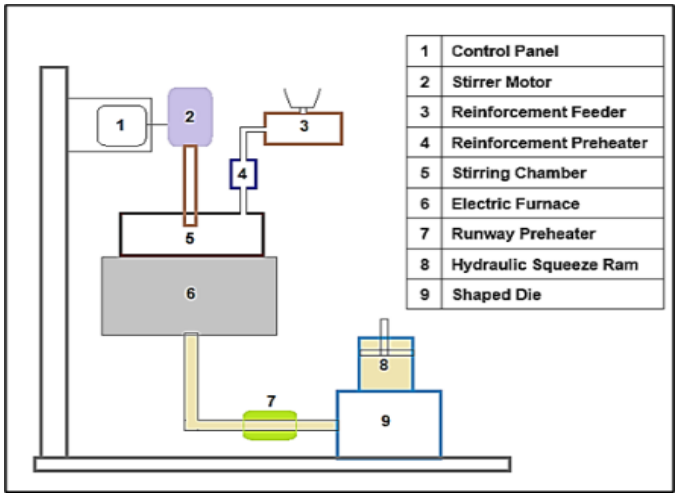

Figure 3. Cross-Sectional View of the Stir Squeeze Casting Machine.

Table 3. Process Parameters of Stir Squeeze Casting Process.

S. No	Process Parameters	Range (Values)
1	Stirring temperature	740 ºC
2	Stirring speed	600 rpm
3	Stirring time	10 mins
4	Preheat temperature of	300 ºC

	reinforcement particles	
5	Preheat temperature of the permanent die	250 ^{o}C
6	Squeeze pressure	75 MPa
7	Matrix material (AL-Si12Fe)	95%
8	Reinforcement material (GO)	5%

Rotational Friction Welding (RFW) machines are sophisticated industrial apparatuses capable of precisely and efficiently joining diverse materials. These devices employ Rotary Friction Welding, a procedure in which one component is rotated at high speeds and forced against a fixed part, generating heat through friction. This technique is very valuable in industries like e-mobility, aerospace, and automotive sectors because it can create parts with complex material combinations, resulting in strong and reliable connections. Figure 4 depicts the arrangement of the RFW machine. The welding process employs a spindle speed of 1400 revolutions per minute (rpm), an upsetting pressure of 150 megapascals (Mpa), an upset pressure of 230 Mpa, and a friction time of 200 seconds.

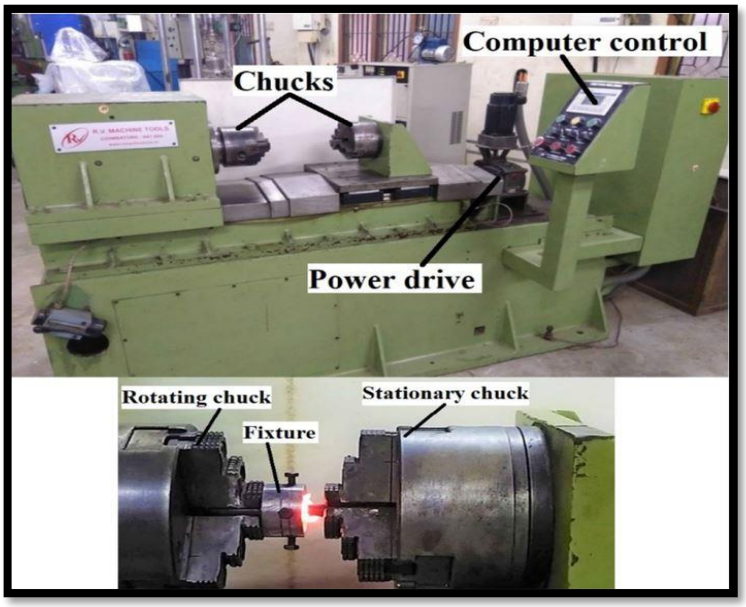

Figure 4. Shows the Layout of FRW [7].

3. Result and Discussion:

The results provided provide an analysis of the mechanical and physical characteristics of four materials: (A) the base material AL-Si12Fe, (B) A with an additional 5% of graphene oxide (GO), (C) A that has undergone welding, and (D) A with an additional 5% of graphene oxide (GO) that has undergone welding.

3.1 Mechanical Characterizations of Composites.

The ASTM standard E-8 was followed in the preparation of each and every sample, and uniaxial tensile testing was carried out on each and every product. Following the measurement of each sample's ultimate tensile strength (UTS) and percentage of ductility, the calculated results were then averaged. For the four samples that are denoted by the letters A, B, C, and D, the stress-strain curves and the average UTS value are depicted in Figure 5. All of the samples are shown in Table 4 with their respective percentage increases in ductility and UTS.

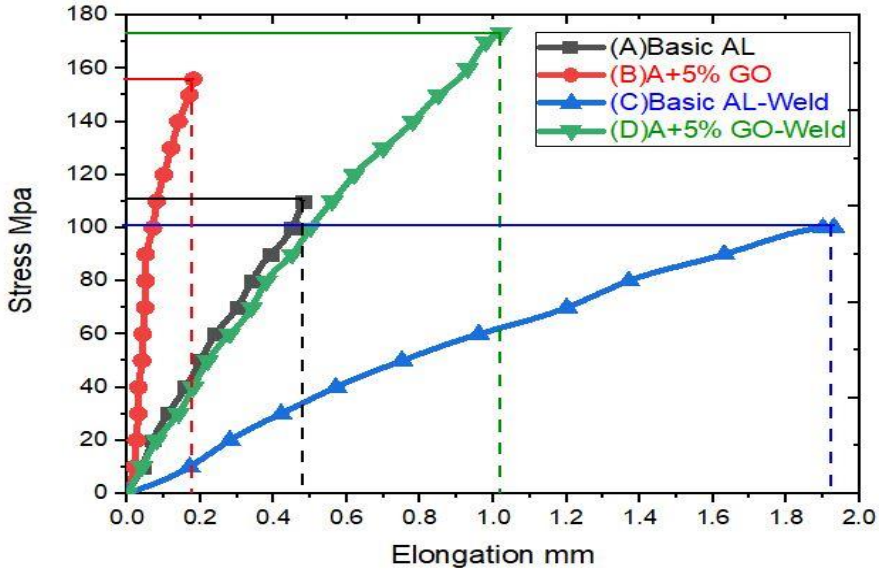

Figure 5. Stress-Strain Curves for Samples A, B, C and D.

Table 4. UTS and Ductility Values of Samples from Tensile Testing.

Sample ID	UTS (MPa)	% UTS	Elongation	% Ductility
A	110	-	0.48	--
B	156	41%	0.18	- 62%
C	100.2	-9 %	1.93	302%
D	173.6	57%	1.02	466%

Friction welding is a method that utilizes severe plastic deformation (SPD) to enhance the crystal microstructure. This procedure facilitates the production of materials with small particle sizes, which is crucial for attaining super-plasticity. Thermomechanical processing, often referred to as recrystallization in the AMC, is another name for this process. We noted a substantial rise in the ductility percentage in the welded samples, peaking at 466%.

Hardness testing using the Vickers method was performed to ascertain the hardness distribution across the composite samples. The hardness testing utilized materials of type (C) and (D). The hardness value of each sample was measured individually, as depicted in Figure 6.

During RFW procedures, the material hardness in the welding zones is reduced compared to

the parent metal due to recovery and recrystallization or removal recrystallization process [8].

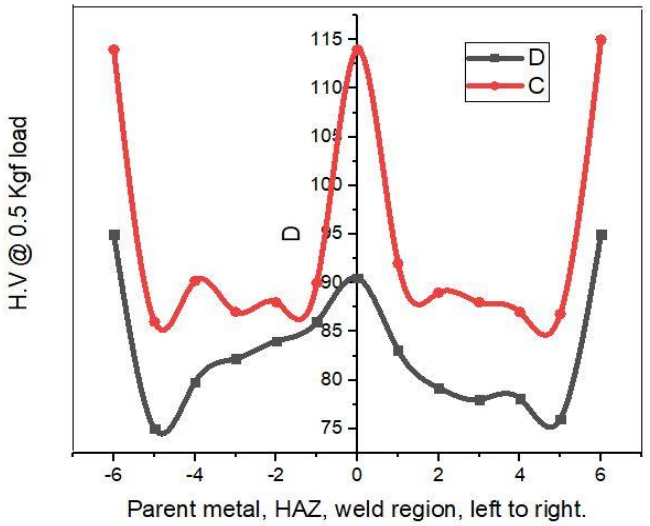

Figure 6. Results of Vickers Hardness Testing

Figure 7 illustrates the energy absorbed by four samples that were prepared according to the ASTM A370 standard.

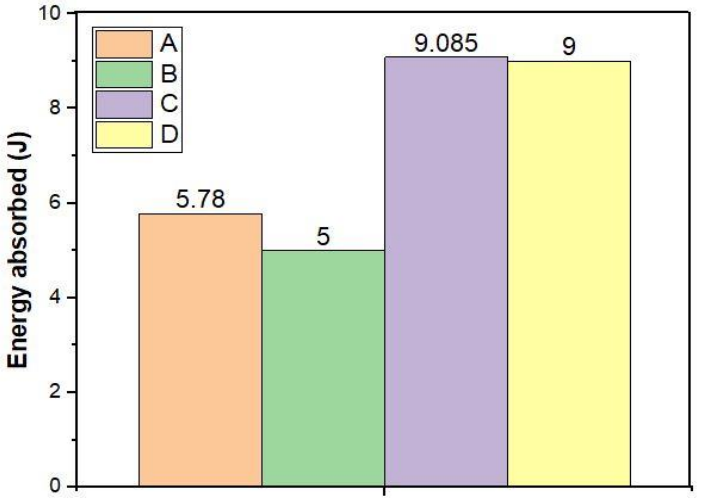

Figure 7. Energy absorbed by impact testing samples.

3.2 Physical Characterizations of Composites.

Figure 8 depicts the microstructural image of an aluminum alloy (AL-Si12Fe). The material is composed of a homogeneous mixture of aluminum and a network of aluminum-silicon eutectic that is found between the dendrites. Figures 9 and 10 depict the microstructure of the heat-affected zone (HAZ) and welding region. Upon meticulous analysis, we saw a reduction

in the dimensions of the particles within the crystals as we transitioned from the heat-affected zone (HAZ) to the welded region. The results suggest that the crystals in the weld region experienced recrystallization due to the super-deformation induced by friction welding procedures [9]. Al, Si, O, C, Fe, and Mg elements were identified in the composite material during the EDS investigation. The elemental maps illustrated in Figure 11.

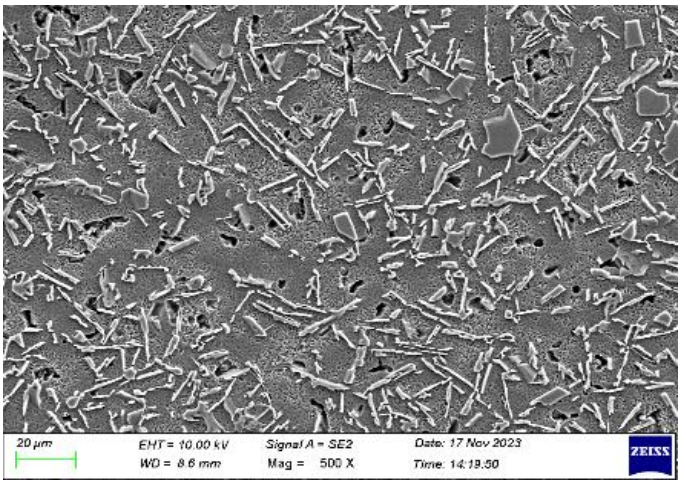

Figure 8. The (AL-Si12Fe) Microstructure.

Figure 9. Sample (C) HAZ.

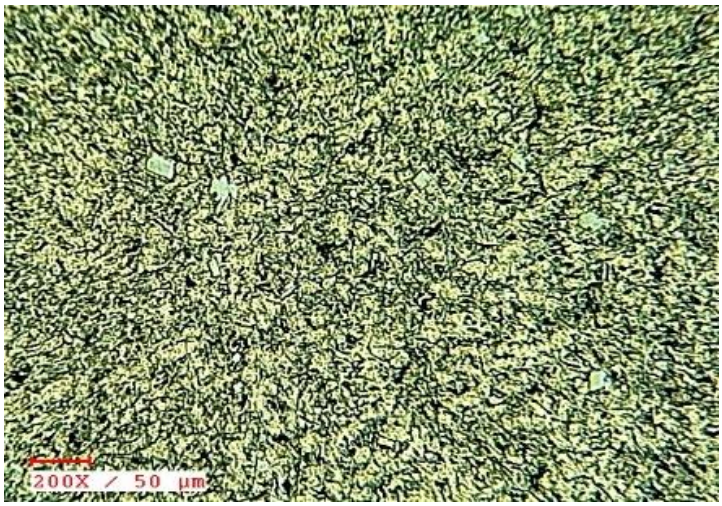

Figure 10. Sample (C) Welding Region.

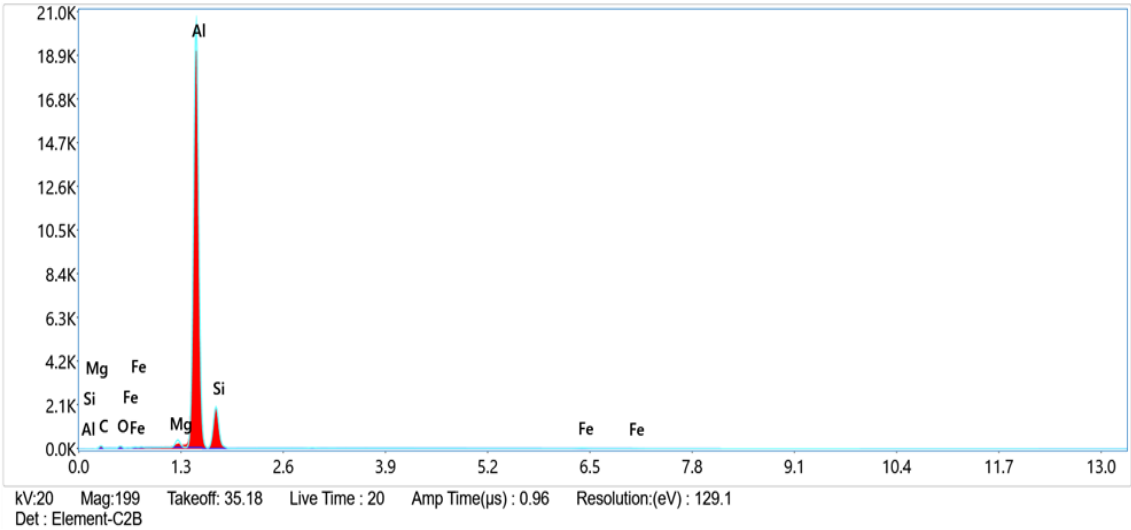

Figure 11. EDS Map of Sample (C) Weld Composite.

Microstructural pictures of the heat-affected zone (HAZ) and welding regions of sample (D) are shown in Figures 12 and 13. Through careful examination, we noticed a decrease in the dimensions of crystal particles from the heat-affected zone (HAZ) to the welded region. The data suggest that friction welding caused significant distortion, resulting in the recrystallization of crystals in the welded region. The EDS examination identified the existence of Al, Si, O, C, Fe, and Mg elements. Figure 14 illustrates the procedure of elemental mapping.

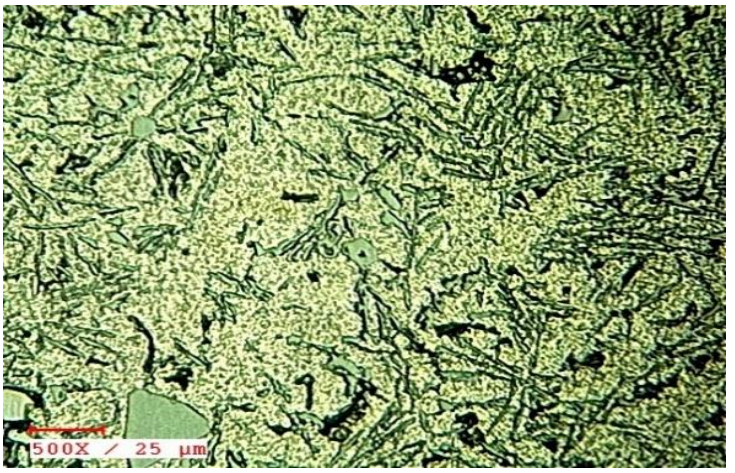

Figure 12. Sample (D) HAZ.

Figure 13. Sample (D) Welding Region.

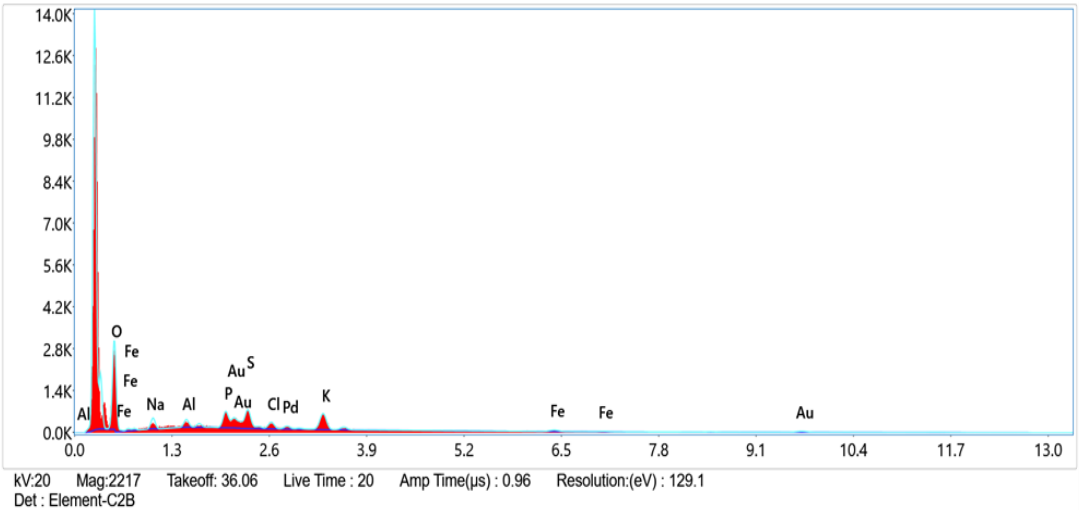

Figure 14. EDS Map of Sample (D) Weld Composite.

4. Conclusion:

- Mechanical tests were conducted on AL-Si12Fe alloy and composites containing 5% GO reinforcements. The results and analysis indicated that the use of GO reinforcements enhanced the mechanical properties of the composite material. The ultimate tensile strength (UTS) of AL-Si12Fe+5%GO and AL-Si12Fe+5%GO-weld composites was 41% and 57% greater, respectively, compared to the base aluminium alloy.

- The application of the rotary friction welding process resulted in a significant increase in ductility, with improvements of 302% and 466% observed, respectively.

- Micrographs and EDS maps were utilized to analyze the morphology of AL-Si12Fe samples containing +5%GO, as well as welded samples from the same user. The study sought to quantify the enhancement of the alloy. The importance of the chemical composition, particle size, and particle size concentration of the reinforcing phase components was shown. The crystal particles underwent shrinkage from the heat-affected zone to the welded area, signifying that the process of friction welding resulted in the crystals undergoing recrystallization in the welded region.

- The adaptable technology of rotary friction welding has the ability to improve crystal characteristics and cause super-deformation.

Acknowledgement:

The authors thank the Centre for Research & Innovation at the National University (NUST), Muscat, Oman, for providing financial assistance.

We express our gratitude to Dr. Saadoon Isaoglu, who serves as the representative of the CDT group, which specializes in the design, manufacturing, and operating services of specialty refineries in Germany and Turkey, for supporting the team.

Funding Statement:

This research was supported by at the National University (NUST), College of Engineering-Oman, Project CFRG-22-0003.

References

1. M. S. Fuhaid, M. A. Maleque, R. V. Murali, and M. A. Rahaman, "Natural and industrial origin reinforced LM6 aluminum matrix composite materials - A comparative study," in AIP Conference Proceedings, American Institute of Physics Inc., May 2022. doi: 10.1063/5.0080174.
2. M. Shafi Fuhaid, P. Kumar Krishnan, and M. Yeakub Ali, "Manufacturing and Friction Welding of Aluminium Matrix Composites-Review of Current Status and Future Directions".
3. M. Sh. Fuhaid, R. V Murali, M. A. Maleque, P. K. Krishnan, and M. A. Rahaman, "Synthesis and Characterization of Aluminium Composite with Graphene Oxide Reinforcement," IOP Conf Ser Mater Sci Eng, vol. 1057, no. 1, p. 012005, Feb. 2021, doi: 10.1088/1757-899x/1057/1/012005.
4. W. S. Hummers and R. E. Offeman, "Preparation of Graphitic Oxide," J Am Chem Soc, vol. 80, no. 6, p. 1339, Mar. 1958, doi: 10.1021/JA01539A017.
5. A. B. Bourlinos, D. Gournis, D. Petridis, T. Szabó, A. Szeri, and I. Dékány, "Graphite oxide: Chemical reduction to graphite and surface modification with primary aliphatic amines and amino acids," Langmuir, vol. 19, no. 15, pp. 6050–6055, Jul. 2003, doi: 10.1021/LA026525H.
6. N. Seyed Pourmand and H. Asgharzadeh, "Aluminum Matrix Composites Reinforced with Graphene: A Review on Production, Microstructure, and Properties," Critical Reviews in Solid State and Materials Sciences, vol. 45, no. 4, pp. 289–337, Jul. 2020, doi: 10.1080/10408436.2019.1632792.
7. T. Dhamothara kannan, P. Sivaraj, V. Balasubramanian, T. Sonar, M. Ivanov, and S. Sathiya, "Unsymmetric rod to plate rotary friction welding of dissimilar martensitic stainless steel and low carbon steel for automotive applications–mathematical modeling and optimization," International Journal on Interactive Design and Manufacturing, 2023, doi: 10.1007/S12008-022-01193-5.
8. A. Heidarzadeh et al., "Friction stir welding/processing of metals and alloys: A comprehensive review on microstructural evolution," Prog Mater Sci, vol. 117, p. 100752, Apr. 2021, doi: 10.1016/J.PMATSCI.2020.100752.
9. P. Geng, G. Qin, H. Ma, J. Zhou, and N. Ma, "Linear friction welding of dissimilar Ni-based superalloys: microstructure evolution and thermo-mechanical interaction," Journal of Materials Research and Technology, vol. 11, pp. 633–649, Mar. 2021, doi: 10.1016/J.JMRT.2021.01.036.